## *Chapter3: Electric circuit model of a myelinated nerve and study of its nerve excitable properties via toad nerve model*

Contents



*If you can dream it, you can do it.*
*-Walt Disney*

## 3.1 Introduction

In multicellular animals, the nervous system is highly complexed in their functions because of the presence of large number of nerve cells or neurons. In case of human nervous system, there are mainly two types of cells- neurons and glia. The human nervous system has $10^{20}$ neurons that are capable of co-coordinating with each other and transmitting sequences of action potential (basically neuro signals) to different parts of the body [1-3]. Glia is mainly responsible to maintain long-term neuronal integrity and providing mechanical and structural strength to the neurons with the inclusion of other functions such as growth factors and insulation around the axons [3-5]. Axons are the fragile and thin cellular extensions of neurons which receive and send signals to other cells in the form of action potentials [6].

The myelin sheaths are basically plasma membrane which wraps round the nerve axon in a spiral fashion [7, 8] which plays important role in propagation of action potential sequences generated by neural membranes. In this direction, reduction of myelin sheaths affect nerve conduction velocity (NCV) where NCV signals obtained from nerve conduction studies are used for clinical analysis of neuro diseases [9]. A layer of Schwann cell membranes of myelinated sheath, grown from the glia cells surrounding the axon plays a crucial role for faster conduction of action potential sequences by saltatory process in which the impulses jump from one node to another via the node of Ranvier [10].

Over the past century, study on the biological system to investigate the mechanism underlying the physiology has become a challenge and an interesting area of research among different research groups. In this context, modeling of the nervous system has been proved to be an important theoretical tool to describe and understand the function and other physiological properties of the nervous system. Keeping all the above considerations in view, this chapter aims to present an electric circuit model of a myelinated nerve considering certain electrical parameters which are responsible for demonstrating physical and thermodynamic properties, essential for appropriate functioning of the nerve impulse of the axons. The chapter also emphasized on both

theoretical results as well as experimental observations obtained from a toad model for its organization, thereby estimating the NCV in a normal peripheral nerve.

## 3.2 Electric circuit modeling of a peripheral myelinated nerve

Mathematical models are developed with the aim to examine the influence of physiological and electrical properties on the functional behavior of excitable nerve fibers. Hodgkin-Huxley (H-H) and Katz developed the computational model to describe the nerve impulse propagation through a nodal membrane [11-13]. Since then, H-H model has been modified subsequently and used successfully to study the nerve excitable properties of a myelinated and unmyelinated nerve fiber [14-16]. In this section, a mathematical model of a myelinated nerve is formulated as shown in Fig-3.1(a) using H-H model to describe nerve conduction properties in a bundle of axons consisting of axon I surrounded by six other axons as shown in Fig-3.1(b) and (c).

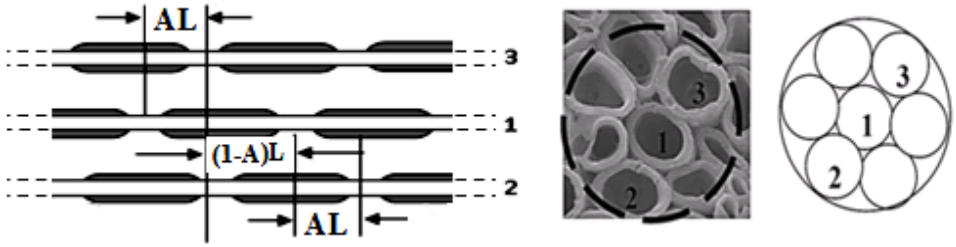


(a) (b (c)

**Figure 3.1**: (a) A bundle of myelinated nerve fibers, (b) SEM image of a bundle of axons in a myelinated nerve and (c) schematic representation of a bundle of axons.

Fig-3.1 (a) represents a bundle of nerve denoting three nerves – nerve 1, nerve 2 and nerve 3 respectively where the Node of Ranvier of axons are misaligned by alignment factor A (where $\frac{1}{2} \leq A \leq 1$). A=1 indicates that two axons are aligned exactly, and A=$\frac{1}{2}$ indicates that two axons are evenly staggered. "L" is the internodal length i.e., the distance between two internodes in the nerve. Fig-3.1(b) is the myelinated nerve image obtained from scanning electron microscope (SEM) denoting a bundle of axons in it. Fig-3.1(c) represents the schematic representation of axon 1 surrounded by six axons of equal diameter corresponding to SEM image.

### 3.2.1. Electric circuit model of a myelinated axon considering a bundle of axons

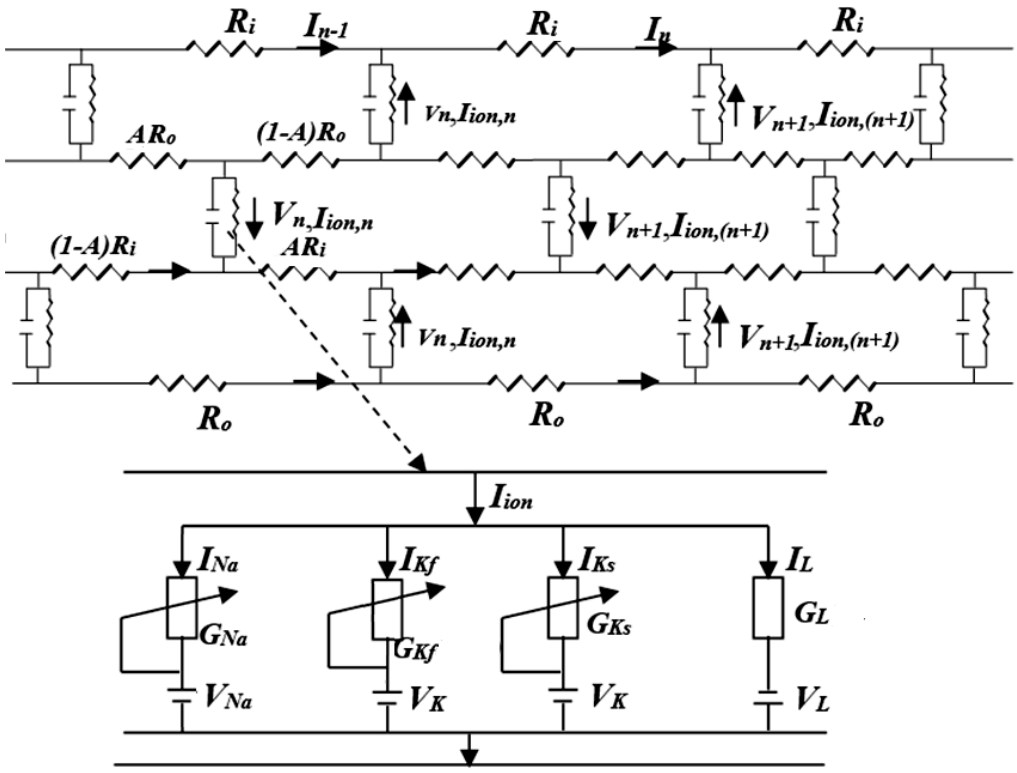


**Figure 3.2**: An equivalent electric circuit of a myelinated nerve fiber.

Fig-3.2 represents an electric circuit model of a peripheral nerve with consisting of an internal resistance of $R_i$ and external resistance of $R_o$, membrane capacitance $C$ and ionic conductance $G_{Na}$, $G_{Kf}$, $G_{Ks}$ and $G_{L,}$ corresponding to sodium ions, fast potassium and slow potassium and leakage ions such as chlorine and calcium ions respectively. In the figure, the index $n$ indicates successive active nodes, each of which is characterized by a transverse (inside to outside) voltage across the membrane ($V_n$). A second dynamic variable is the current ($I_n$) flowing longitudinally through the fiber from node $n$ to node $n+1$. The total ionic current at node n in a myelinated nerve in human is represented by

$$I_{ion,n} = I_{Na,n} + I_{Kf,n} + I_{Ks,n} + I_{L,n} \tag{3.1}$$

The currents can be written in terms of conductance and potential (as shown in Fig-3.2) with cubic polynomial function approximation [17] and considering resting potential zero at equilibrium as

$$I_{Na,n} = \left(\frac{G_{Na}}{V_{Na}(V_{Na} - V_{th}^{Na})}\right) V_n (V_n - V_{th}^{Na})(V_n - V_{Na})$$

$$I_{Kf,n} = \left(\frac{G_{Kf}}{V_K (V_K - V_{th}^{Kf})}\right) V_n (V_n - V_{th}^{Kf})(V_n - V_K)$$

$$I_{Ks,n} = \left(\frac{G_{Ks}}{V_K (V_K - V_{th}^{Ks})}\right) V_n (V_n - V_{th}^{Ks})(V_n - V_K)$$

$$I_{L,n} = \left(\frac{G_L}{V_L (V_L - V_{th}^{L})}\right) V_n (V_n - V_{th}^{L})(V_n - V_L) \quad (3.2)$$

Where $V_n$ is the voltage at node $n$. $V_{th}^{Na}$, $V_{th}^{Kf}$, $V_{th}^{Ks}$ and $V_{th}^{L}$ are the threshold voltage of sodium, fast potassium, slow potassium and leakage component respectively, at which sodium, fast potassium, slow potassium and leakage current begins to flow into an active node. $V_{Na}$, $V_K$ and $V_L$ are Nernst (diffusion) potentials at which the ionic currents for sodium, fast potassium, slow potassium and leakage current returns to zero respectively. $I_{Na}$, $I_{Kf}$, $I_{Ks}$ and $I_L$ are the ionic currents responsible mainly due to flow of sodium, fast potassium, slow potassium and other ions known as the leakage currents.

## 3.2.2. Formulation of NCV in the modeled myelinated nerve

In this section nerve conduction value is estimated by using electrical circuit model as shown in Fig-3.2. Applying Kirchoff's voltage law, the current at node n-1 and node n can be written as

$$I_{n-1} = (V_{n-1} - V_n)/(R_i + R_o) \quad (3.3)$$

$$I_n = (V_n - V_{n+1})/(R_i + R_o) \quad (3.4)$$

From Kirchoff's current law, the current at the nodes can be written as

$$I_{n-1} - I_n = C\frac{\partial V_n}{\partial t} + I_{ion,n} \tag{3.5}$$

Using equation (3.3), (3.4) and (3.5), it can be written as

$$(V_{n-1} - V_n)/(R_i + R_o) - (V_n - V_{n+1})/(R_i + R_o) = C\frac{\partial V_n}{\partial t} + I_{ion,n} \tag{3.6}$$

Considering total resistance of nerve fiber $R = R_i + R_o$, equation (3.6) becomes

$$1/R\,[V_{n-1} - 2V_n + V_{n+1}] = C\frac{\partial V_n}{\partial t} + I_{ion,n} \tag{3.7}$$

Using equation (3.2), equation (3.7) can be written as

$$\begin{aligned} 1/R\,[V_{n-1} - 2V_n + V_{n+1}] = C\frac{\partial V_n}{\partial t} &+ \left(\frac{G_{Na}}{V_{Na}(V_{Na} - V_{th}^{Na})}\right)V_n(V_n - V_{th}^{Na})(V_n - V_{Na}) \\ &+ \left(\frac{G_{Kf}}{V_K(V_K - V_{th}^{Kf})}\right)V_n(V_n - V_{th}^{Kf})(V_n - V_K) \\ &+ \left(\frac{G_{Ks}}{V_K(V_K - V_{th}^{Ks})}\right)V_n(V_n - V_{th}^{Ks})(V_n - V_K) \\ &+ \left(\frac{G_L}{V_L(V_L - V_{th}^{L})}\right)V_n(V_n - V_{th}^{L})(V_n - V_L) \end{aligned} \tag{3.8}$$

Replacing *1/RC* by *D*, where *D=1/RC* is a diffusion constant in squared centimeters per second$^2$ in equation (3.8), then, in this formulation, the dynamic equation becomes

$$D[V_n - 2V_n + V_{n+1}] = \frac{\partial V_n}{\partial t} + {}^{1}\!/_{C}\left[\left(\frac{G_{Na}}{V_{Na}(V_{Na} - V_{th}^{Na})}\right)V_n(V_n - V_{th}^{Na})(V_n - V_{Na})\right.$$

$$+\left(\frac{G_{Kf}}{V_K(V_K - V_{th}^{Kf})}\right)V_n(V_n - V_{th}^{Kf})(V_n - V_K)$$

$$+\left(\frac{G_{Ks}}{V_K(V_K - V_{th}^{Ks})}\right)V_n(V_n - V_{th}^{Ks})(V_n - V_K)$$

$$+\left(\frac{G_L}{V_L(V_L - V_{th}^{L})}\right)V_n(V_n - V_{th}^{L})(V_n - V_L)] \tag{3.9}$$

The equation (3.9) represents a discrete reaction diffusion equation of myelinated nerve. Since internodes' spacing is very small, the continuum limit is reached [18]. So equation (3.9) can be written in continuum limit as partial differential equation which is given below,

$$D\frac{\partial^2 t}{\partial x^2} - \frac{\partial V}{\partial t} = 1/C[\left(\frac{G_{Na}}{V_{Na}(V_{Na} - V_{th}^{Na})}\right)V_n(V_n - V_{th}^{Na})(V_n - V_{Na})$$

$$+\left(\frac{G_{Kf}}{V_K(V_K - V_{th}^{Kf})}\right)V_n(V_n - V_{th}^{Kf})(V_n - V_K)$$

$$+\left(\frac{G_{Ks}}{V_K(V_K - V_{th}^{Ks})}\right)V_n(V_n - V_{th}^{Ks})(V_n - V_K)$$

$$+\left(\frac{G_L}{V_L(V_L - V_{th}^{L})}\right)V_n(V_n - V_{th}^{L})(V_n - V_L)] \tag{3.10}$$

In 1938, Zeldovich and Frank Kamenetsky [19] first obtained the equation for conduction speed to be $v_c = \sqrt{g/rc^2}$ **,** where the distance is measured in units of $1/\sqrt{rg}$ and time in units of c/g. Later, it is translated into the notation

$$v_c = \sqrt{\frac{g}{rc^2}} \frac{V_2 - 2V_1}{\sqrt{2V_2}} \tag{3.11}$$

where,

$$f(V) = \frac{V(V - V_1)(V - V_2)}{V_2(V_2 - V_1)} \tag{3.12}$$

In equations (3.11) and (3.12), $r$ and $c$ are the resistance and capacitance of a single axon and $g$ is the conductance of sodium ion in the axon. $V_1$ is threshold voltage and $V_2$ represents the Nernst potential for sodium ion. For a bundle of nerves, total resistance, $R=R_i+R_oA(N-1)$ and coupling constant, α in terms of alignment factor $A$, respective internal resistance normal nerve $R_i$ and external resistance of normal nerve $R_o$ and number of axons $N$ in the bundle is given by

$$\alpha = \frac{R_i}{R_i + R_o A(N-1)} \tag{3.13}$$

Therefore, the equivalent resistance in the bundle becomes

$$R = \frac{R_o A(N-1)}{(1-\alpha)} \tag{3.14}$$

Using traveling wave solutions of equation (3.10) with leading edge approximation [20] for action potential pulse and replacing $D$ by $1/RC$, the conduction velocity of a myelinated nerve in terms of coupling constant and alignment factor in a bundle from the electric circuit model shown in Fig-3.2 is obtained as

$$v_c = \sqrt{\frac{G_{Na}(1-\alpha)}{R_o A(N-1)C^2}} \left(\frac{V_{Na} - 2V_{th}^{Na}}{\sqrt{2V_{Na}}}\right) + \sqrt{\frac{G_{Kf}(1-\alpha)}{R_o A(N-1)C^2}} \left(\frac{V_K - 2V_{th}^{Kf}}{\sqrt{2V_K}}\right)$$

$$+\sqrt{\frac{G_{Ks}(1-\alpha)}{R_O A(N-1)C^2}}\left(\frac{V_K-2V_{th}^{Ks}}{\sqrt{2V_K}}\right)+\sqrt{\frac{G_L(1-\alpha)}{R_O A(N-1)C^2}}\left(\frac{V_L-2V_{th}^{L}}{\sqrt{2V_L}}\right) \quad (3.15)$$

**Table 3.1**: Standard parameters for normal peripheral nerve [10, 21]

| Parameters | Values |
|---|---|
| Internal Resistance ($R_i$) | 88.30 MΩ |
| External Resistance ($R_o$) | 10 MΩ |
| Capacitance ($C$) | 388.5 pF |
| Sodium conductance ($G_{Na}$) | 26 nS |
| Fast potassium conductance ($G_{Kf}$) | 15 nS |
| Slow potassium conductance($G_{Ks}$) | 30 nS |
| Leakage conductance ($G_L$) | 30 nS |
| Nernst sodium potential ($V_{Na}$) | 61.5 mV |
| Nernst potassium potential ($V_K$) | -84 mV |
| Leakage potential ($V_L$) | -84 mV |
| Sodium threshold potential ($V_{th}^{Na}$) | -70 mV |
| Fast potassium threshold potential ($V_{th}^{Kf}$) | -70.2 mV |
| Slow potassium threshold potential ($V_{th}^{Ks}$) | 69.8 mV |
| Leakage threshold potential ($V_{th}^{L}$) | 70 mV |

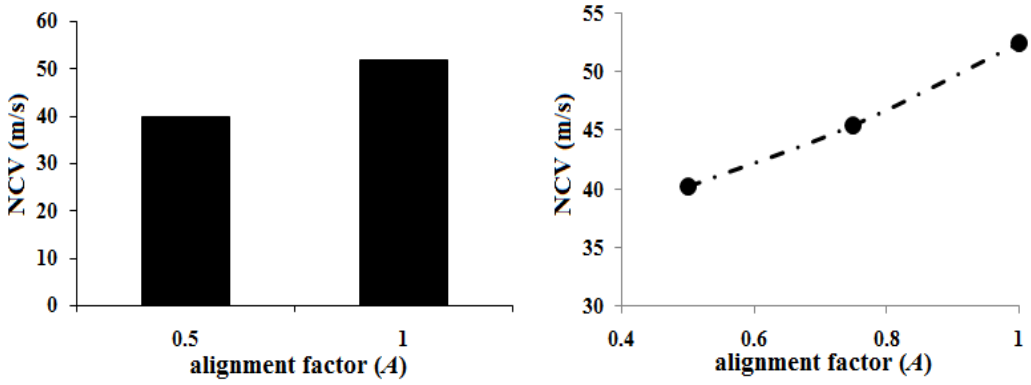


(a) (b)

**Figure 3.3**: (a) Estimation of NCV in terms of alignment factor and (b) variance of NCV with increasing alignment of axons in the bundle.

Fig-3.3(a) represents the variation of NCV with the alignment factor ($0.5 \leq A \leq 1$) in the bundle of axons present in the myelinated peripheral nerve. It is seen that NCV in exactly aligned bundle of axons ($A=1$) is more in comparison to that of misaligned bundle of axons ($A=1/2$). The NCV seems to increase linearly as the bundle in the nerve tends to have higher values of alignment as seen in Fig-3.3(b). Thus NCV depends on the degree of alignment patterns of axons in a bundle of myelinated nerves.

## 3.3 Experimental validation *via* toad nerve model

Experimental validation in neurobiology is a special type of biomedical experimentation with the practice of using animal models to study and validate the pathophysiology, symptomatology and response to therapeutic inventions. The validation process with the use of animal models includes theoretical formulations of an algorithm and predictive calculations of a number of statistical parameters for a biological model under human environmental conditions. In this section, the theoretical formulation is validated with a toad model by recording the electric nerve conduction signals externally in its isolated sciatic nerves.

### 3.3.1 Materials

In this section, the chemicals and reagents used to perform the experiments are discussed. All the reagents are of analytical grade.

### 3.3.1.1 Reagents

Ringers solution (NaCl- 118.4mM, KCl- 4.7mM, $MgSO_4$- 1.2mM, $KH_2PO_4$- 1.2mM, $CaCl_2$- 2.5mM, $NaHCO_3$- 25mM, Glucose- 11.1mM) is used for nerve tissue storing and performing experiment. Ethanol is used for cleaning instruments and working place.

### 3.3.1.2 Animals

Common Asian toads (*Duttaphrynus melanostictus*) of same age (~1-2 months) are used as an animal model to perform the validation experiments. Sciatic nerves of the collected toads are isolated and used for validation of NCV and calibrating compound action potential (CAP) recordings. The experiments on toads are performed 5-6 times and standard deviation (SD) is estimated to minimize the percentage of error during the experiments.

**Figure 3.4**: *Duttaphrynus melanostictus*

### 3.3.1.3 Instrumental set up

Extracellular recordings are performed in an instrument known as the AD instrument. The instrument consists of a nerve chamber equipped with 15 stainless steel electrodes as shown in Fig-3.5. A dual Bio Amp/stimulator is used to obtain and record CAP. The set up is comprised of a set of stimulating and recording cable and two male BNC (Bayonet Neill–Concelman) connectors to three micro-hooks constructed of gold-plated beryllium copper which is used to stimulate the nerve.

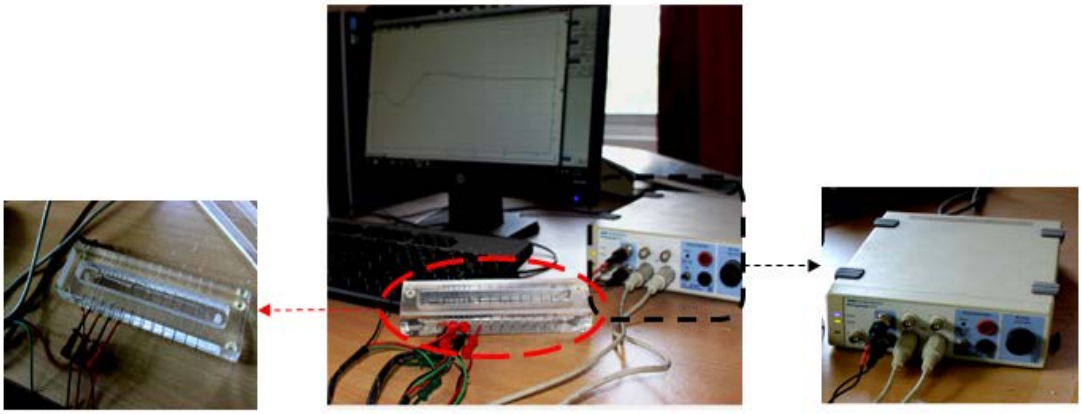

**Figure 3.5**: AD instrument with nerve chamber used to record nerve signals.

## 3.3.2 Methods

All animal experiments are performed in accordance with the guidelines from the Defence Research Laboratory, Tezpur, Assam (India) under Registration Number 1227/bc/07/CPCSEA and approved by Tezpur University Animal Ethical Committee (TUAEC) (Approval no : DORD-Pro/TUAEC/10-56/14/Res-06). The entire experimental procedure emphasizes to minimize both animal sufferings as well as number of animals used for the purpose.

### 3.3.2.1 Isolation of sciatic nerves

The method as described by Katsuki et al. is followed for sciatic nerve preparation [22]. In brief, common Asian toads *(Duttaphrynus melanostictus)* weighing 30-35gm of either sex are decapitated and then pithed. Sciatic nerve of length 4-6cm and 0.5-1mm diameter is dissected from lumber plexus to the knee joint. Throughout the procedure the nerve is continuously flooded with Ringer's solution. Finally, the dissected nerve is mounted on nerve chamber (AD Instruments, Powerlabs, Australia) containing Ringer's solution.

### 3.3.2.2 Recording of CAPs and estimation of NCV from the prepared sciatic nerves

Standard techniques for extracellular recordings were followed. CAP is measured in a nerve chamber (AD Instruments, Powerlabs, Australia). In brief, the dissected sciatic nerve is externally stimulated with a frequency of 1Hz where pulses at 0.1ms duration are used to determine the CAP [22]. The electrodes for proximal and distal stimulus

recording are placed at a distance of 3cm. Nerve end with lumber plexus of spinal cord is connected with proximal recording electrode and electrode at nerve end connecting knee joint acted as distal recording electrode. Each experiment for recording of CAP is completed within 20s of timeframe to avoid drying of the dissected nerve. CAP is analyzed by SCOPE (Powerlabs, Australia). The experiments are performed six times and standard deviation (SD) is estimated to minimize the percentage of error as per standard method. The NCV is calculated using the latency difference between the proximal and distal ends of the nerve and distance data from the signal as shown in Fig-3.6, where latency is the time taken to conduct action potential from the stimulating source to the recording electrodes and distance represents the length between the electrodes placed at distal and proximal ends of the isolated nerve fiber.

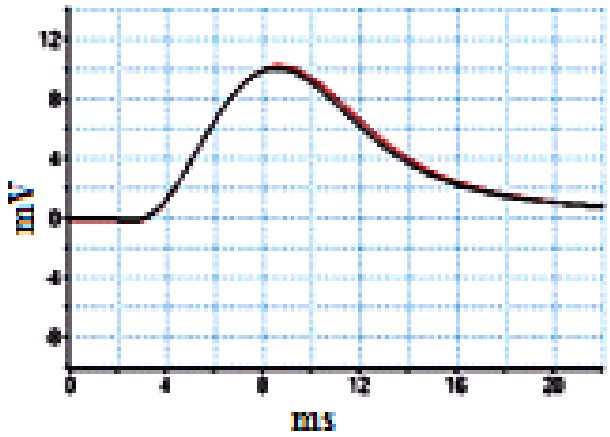


**Figure 3.6**: Electric neuro signal of a normal sciatic nerve of toad.

### 3.3.2.3 Scanning Electron Microscope (SEM) imaging

Sciatic nerves are subjected for SEM analysis to check the effect of crude venom on morphology of the isolated nerve. Sciatic nerve preparations are incubated for 15mins before fixation is performed on the prepared isolated sciatic nerves of toad. Firstly, the nerves are subjected to primary fixation using 2.5% gluteraldehyde for 4hr followed by secondary fixation using 1% $OsO_4$ (Osmium tetroxide) for 4hr for better penetration. Cross section of sciatic nerve is made by slicing at a length of 10mm using glass cutter in a microtome for maintaining uniformity. The sliced nerve segments are further observed under SEM for the structural change. The thickness of myelin in the isolated

nerves considering 6-7 nerves in a bundle is quantified with the use of measuring scale installed in the SEM.

## 3.4 Results

The formulation for the determination of NCV is simulated in MATLAB. The value of NCV estimated from the formulation using equation (3.15) and by considering parameters of normal nerve (Table 3.1) are found to be 40.21m/s and 52.18m/s in misaligned and aligned bundles which are within the normal range of 35-65m/s obtained from literature survey reports.

**Table 3.2**: Estimation of NCV (m/s) and myelin thickness (μm) in normal sciatic nerve of toad

| No. of observations | Experimental observations | |
|---|---|---|
| | NCV (m/s) | Myelin thickness (μm) |
| **I** | 32.78 | 1.79 |
| **II** | 33.14 | 1.79 |
| **III** | 33.07 | 1.83 |
| **IV** | 32.99 | 1.85 |
| **V** | 32.81 | 1.75 |
| **VI** | 32.85 | 1.73 |
| **SD** | 32.90±0.21 | 1.79±0.05 |

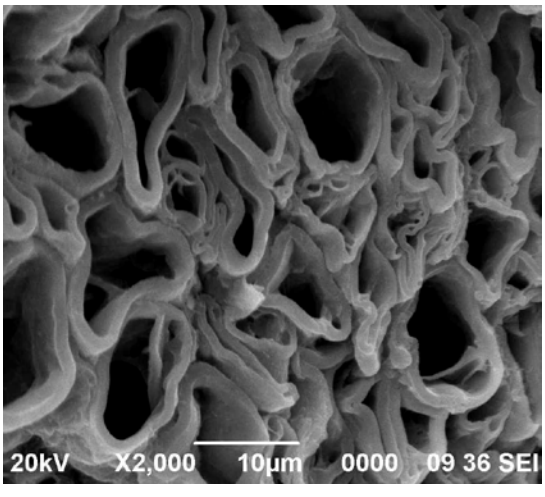


**Figure 3.7**: SEM image of a myelinated nerve fiber.

The propagation of action potential stimuli applied on sciatic nerves is estimated experimentally to validate the theoretical results. The NCV is determined by using distance between two electrodes and divided by latency between proximal and distal action potential (shift between peaks of proximal and distal action potential) as 32.90±0.21m/s which is a normal NCV in case of toad as shown in Fig-3.5 and Table-3.2, matches well with the theoretical results. Moreover, SEM image of myelinated sciatic nerves of toad witnesses a normal myelin thickness of 1.79±0.05μm (obtained from Fig-3.6 and Table-3.2).

## 3.5 Discussions

It is seen that the conduction speed of an impulse in a myelinated nerve is directly proportional to the fiber diameter. The nodes present in a nerve fiber with larger diameter conducts nerve signals with greater efficiency due to the presence of myelin sheaths. So the NCV is greater in case of a myelinated nerve in comparison to that of an unmyelinated nerve fiber. In the human body, activated gate of voltage-gated sodium channel and the two activated gates of potassium channel due to fast $K^+$ and slow $K^+$ ions are responsible for generation of action potential and conduction of nerve impulse through the channels. Apart from these two channels, there is a leakage channels for the entry and exit of ions such as $Cl^-$ and $Ca^{2+}$ which also plays a significant role in nerve conduction. The value of NCV and the peaks of amplitude of action potential estimated from the repetition of the validation experiments with toad's sciatic nerve presented almost similar results all the time, indicating the correctness of the experiment.

## 3.6 Conclusion

In the proposed work, an electric circuit model of a myelinated peripheral nerve consisting of a bundle of axons is designed successfully by providing equal importance on the electrical parameters such as resistance, capacitance and respective ionic conductances responsible for nerve conduction by the movement of ions through the ionic channels. A coupling constant and an alignment parameter were also considered in the bundled nerve to design the proposed model. The NCV estimated theoretically by using the electric circuit model of a peripheral myelinated nerves consisting of a bundle

of axons are 40.21m/s and 52.18m/s in scattered and evenly aligned bundle of axons. The NCV calculated from the repeated experiments on sciatic nerve of toad is found to be 32.90±0.21m/s which is a normal value in case of toad nerve model with a normal myelin thickness of 1.79±0.05μm as obtained from SEM image. However, theoretical results which are based on human data obtained from literature works possess higher values of NCV than that of the experimental results performed on toad model. This mismatch is due to nerve function estimation parameters such as axon diameter, length of the nerve, etc. are higher in case of human in comparison to a toad. As a result, NCV in human are greater than that of a toad as witnessed in the theoretical and experimental results respectively. All the electrical components have its own specific role in nerve conduction. So, it is important to take into account of all the components/parameters in order to proceed for further modeling of any disordered nerves for its diagnosis and therapeutic processes.

# Bibliography

[1] Brown, A, G. Introduction to nerve cells and nervous systems. In *Nerve cells and nervous systems: an introduction to neuroscience,* pages 1-14, ISBN:978-3-540-76090-0, Springer-Verlag, London, 2001.

[2] Chang, K. J., Redmond, S. A., and Chan, J. R. Remodeling myelination: implications for mechanisms of neural plasticity. Nature Neuroscience, 19(2):190-197, 2016. DOI:10.1038/nm.4200.

[3] Susuki, K. Myelin: A specialized membrane for cell communication, *Nature Education* 3 (9):59, 2010.

[4] Waxman S.G. Axon-glia interactions: building a smart nerve fiber. *Current Biology*, 7:R406-R410, 1997.

[5] Eshed-Eisenbach, Y. and Peles, E. The making of a node: a co-production of neurons and glia. *Current Opinion in Neurobiology*, 23:1049-1056, 2013.

[6] Monsivais, P., Clark, B. A., Roth, A. and Häusser, M. Determinants of Action Potential Propagation in Cerebellar Purkinje Cell Axons. *Journal of Neuroscience*, 25(2):464-472, 2005.

[7] Zalc, B., Goujet, D., and Colman, D. The origin of the myelination program in vertebrates. *Current Biology,* 18:R511–R512, 2008.

[8] Jessen, K. R. and Mirsky, R. The origin and development of axon ensheathment and myelin growth. *Nature Reviews Neuroscience*, 6:671-690, 2005.

[9] Waxman, S. G. Determinants of conduction velocity in myelinated nerve fibers. Muscle & Nerve, 3:141-150, 1980.

[10] Schwarz, J. R., Reid, G. and Bostok, H. Action potentials and membrane currents in the human node of Ranvier. *Journal of Physiology,* 430:283-292, 1995.

[11] Hodgkin, A. L. and Huxley, A. F. A quantitative description of membrane and its application to conduction and excitation in nerve. *Journal of Physiology*, 117:500-544, 1952.

[12] Hodgkin. A. L. and Huxley, A. F. The components of membrane Conductance in the giant axon of Loligo. *Journal of Physiology*, 116:473-496, 1952.

[13] Hodgkin, A. L. and Katz, B. The effect of sodium ions on the electrical activity of the giant axon of the squid. *Journal of Physiology*, 108:37-77, 1949.

[14] Koles, Z. L. and Rasminsky, M. A computer simulation of conduction in demyelinated nerve fibers. *Journal of Physiology*, 227:351-364, 1972.

[15] Schnabel, V. and Johannes, J. S. Evaluation of the Cable Model for Electrical Stimulation of unmyelinated Nerve Fibers. *IEEE transaction on Biomedical Engineering*, 48(9):1027-1033, 2001.

[16] Tai, C., Groat, W. C., and Roppolo, J. R. Simulation analysis of conduction block in unmyelinated axons induced by high-frequency biphasic electrical currents. *IEEE transaction on Biomedical Engineering*, 52(7):1323-1332, 2005.

[17] Binczak, S., Eilbeck, J. C., and Scott, A. C. Ephaptic coupling of myelinated nerve fibers. *Physica D: Nonlinear Phenomena*, 148:159-174, 2011.

[18] Scott, A. Myelinated Nerves. In Neuroscience: A mathematical premier, pages 139-147, ISBN:0-387-95403-1. Springer-Verlag, 2002.

[19] Zeldovich, Y. B. and Kamenetsky, F. teorii ravnomernogo rasprostranenia plameni (Toward a theory of uniformly propagating flames). *Doklady Akademii Nauk SSSR*, 19:693-697, 1938**.**

[20] Rissman, P. The leading edge approximation to the nerve axon problem. *Bulletin of mathematical biology*, 39:43-58, 1977.

[21] Stephanova, D. L., Daskalova, M. S., and Alexandrov, A. S. Differences in membrane properties in simulated case of demyelinating neuropathies, internodal focal demyelination with conduction block. *Journal of Biological physics*, 32:129-144, 2006.

[22] Katsuki, R., Fujita, T., Kogra, A., Liu, T., Nakatsuka, T., Nakashima, M., and Kumamota, E. Tramadol, but not its major metabolite (mono-O-demethyl tramadol) depresses compound action potentials in frog sciatic nerves. *British Journal of Pharmacology*, 149:319-327, 2006.